Dalton Transactions

PAPER

View Article Online
View Journal | View Issue

Cite this: *Dalton Trans.*, 2016, **45**, 7998

Identification of Zr(IV)-based architectures generated from ligands incorporating the 2,2′-biphenolato unit†

Chengrui Miao, Georges Khalil, Alain Chaumont, Pierre Mobian* and Marc Henry

Received 2nd February 2016,
Accepted 22nd March 2016

DOI: 10.1039/c6dt00471g

www.rsc.org/dalton

The structural identification in solution of the Zr(IV) complexes involving two 2,2-biphenol-based proligands is reported. The proligand L^1H_2 contains one 2,2-biphenol unit whereas L^2H_4 incorporates two 2,2-biphenol units linked by a *para*-phenylene bridge. Diffusion Ordered Spectroscopy (DOSY) combined with electrospray mass spectrometry analysis and density functional theory (DFT) allowed for determining the molecular structures of such Zr(IV)-based architectures. It is proposed that $[Zr(OPr^i)_4(HOPr^i)]$ in the presence of L^1H_2 generates an octahedral complex formulated as $[ZrL^1{}_3H_2]$. Concerning the self-assembled architecture incorporating the L^2 ligand, the analytical data highlight the formation of an unprecedented neutral Zr(IV) triple-stranded helicate ($[Zr_2L^2{}_3H_4]$). Insight into the geometry of these complexes is obtained *via* DFT calculations. Remarkably, the helicate structure characterized in solution strongly contrasts with the triple-stranded structure of the complex that crystallizes.

Metal alkoxides or aryloxides are a major class of compounds that are extensively employed as precursors for sol–gel chemistry and materials science.[1] Their chemistry is recognized as being highly complex since the predictable synthesis of complexes starting from these metallic precursors is extremely challenging. Undoubtedly, this complex chemistry arises from the singular reactivity of metal alkoxide or aryloxide complexes. Metal alkoxide or aryloxide species display generally complex behaviours in solution owing to their strong tendencies for oligomerisation *via* the formation of oxo, hydroxo and/or alkoxo-bridges between metals leading to solid-state molecular structures that are frequently far from those expected for complexes in solution.[2] Recently, we have demonstrated the possibility of incorporating biphenolate-Ti(IV) motifs in a predictable way into self-assembled molecular structures. The rational approach adopted by our group has permitted us to generate helical architectures starting from titanium isopropoxide and a zig-zag strand incorporating two 2,2′-biphenol units. In order to extend this metallo-supramolecular chemistry to other metal alkoxide precursors, we describe in this manuscript the coordination chemistry involving substituted 2,2′-biphenol ligands with the Zr(IV) centre.

In this manuscript we report the liquid state characterisation of the architectures resulting from the reactions of the Zr(IV) centre with 2,2′-biphenol-based compounds. The proligands L^1H_2 and L^2H_4[3] involved in this study are depicted in Fig. 1. As mentioned above, this set of 2,2′-biphenol derivatives has been shown to generate complex controlled assemblies in the presence of the Ti(IV) centre. For instance, L^1H_2 leads to a monomeric C_2-symmetric complex constructed around an octahedral titanium centre. This compound is formulated as $[Ti(L^1)_2(HOPr^i)_2]$.[4] Concerning the strand L^2H_4, helical neutral assemblies named $[Ti_3(L^2)_3(HOPr^i)_6]$ and $[Ti_2(L^2)(L^2H)(OPr^i)(HOPr^i)_2]$ were characterised.[5] Having proved that these ligands are well suited for displaying a rich Ti(IV) coordination chemistry, we examine now the role of the metal ion size on the resulting assemblies. Thus, it appeared to us particularly relevant to study the coordination chemistry of these two compounds, *i.e.* L^1H_2 and L^2H_4 in the presence of zirconium(IV). Compared to Ti(IV), Zr(IV) is known for being bigger with a Pauling ionic radius ratio between Zr(IV) and Ti(IV) equal to

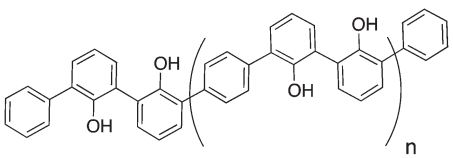

Fig. 1 Compounds L^1H_2 and L^2H_4.

Laboratoire de Chimie Moléculaire de l'Etat Solide (Chimie de la Matière Complexe, UMR 7140), Université de Strasbourg, 67070 Strasbourg, France.
E-mail: mobian@unistra.fr

† Electronic supplementary information (ESI) available. CCDC 1451432. For ESI and crystallographic data in CIF or other electronic format see DOI: 10.1039/c6dt00471g

r(Zr(IV))/r(Ti(IV)) = 1.15.[6] Thus, Zr(IV)-complexes with coordination numbers higher than six are rather common in comparison with Ti(IV)-complexes.[7] Also, the large ionic radius of Zr(IV) permits accommodation of bulky ligands around this metallic centre.[8]

Hereafter, we report the methodology allowing to elucidate the formula of the compounds resulting from the reactions of L^1H_2 or L^2H_4 with Zr(IV). We show that DOSY supported by mass spectrometry analysis and DFT calculations are a key combination to elucidate the nature of these species formed *in situ*. This study shows that the structures incorporating the Zr(IV) ions are dissimilar from those already mentioned for Ti(IV). In particular, this investigation highlights that Zr(IV) accommodates three bidentate oxygenated L^1 ligands. This particular feature allows the formation of an assembly composed of two Zr(IV) centres and three strands when Zr(IV) reacts with L^2H_4. DFT calculations suggest for the dinuclear assembly a triple-stranded helicate structure formulated as $Zr_2L^2{}_3H_4$. Finally, we show that this metallo-supramolecular chemistry conducted with Zr(IV) and L^2H_4 generates in the solid state an assembly strongly dissimilar from the one characterized in solution.

Results and discussion

$ZrL^1{}_3H_2$

The zirconium source employed to conduct this study was the "classical" $[Zr(OPr^i)_4(HOPr^i)]$ alkoxide complex. It is noteworthy that this species adopts a dimeric structure involving di-μ-isopropoxo bridges ($[Zr_2(OPr^i)_8(HOPr^i)_2]$) in solution and in the solid state with two intramolecular hydrogen bonds characterized for this compound.[9] First, several reaction conditions were tested by reacting $[Zr(OPr^i)_4(HOPr^i)]$ with 1, 2 and 3 equivalents of L^1H_2 in CD_2Cl_2. The resulting uncoloured mixtures were analysed by ^{1}H NMR (see the ESI†). Surprisingly, these coordination reactions were not efficient as the L^1H_2 compound was largely predominant in solution for the three molar ratios tested. Also, the final composition of these mixtures was not really affected when these samples were heated. The most promising result was obtained when $[Zr(OPr^i)_4(HOPr^i)]$ reacted with two equivalents of L^1H_2. New large signals different from those observed for the initial components were clearly identified by ^{1}H NMR as shown in Fig. 2, highlighting the formation of a Zr-based complex. A conversion ratio of about 51% could be estimated by ^{1}H NMR after integration of the most deshielded signal of the unreacted L^1H_2 and the methine proton signal (δ = 3.93 ppm, broad signal). We explain this conversion by the dimeric structure of $[Zr_2(OPr^i)_8(HOPr^i)_2]$ rendering this precursor moderately reactive.[1] The aliphatic region of the ^{1}H NMR spectrum displays two intense very broad resonances at δ = 3.89 ppm and 1.09 ppm (see the ESI†). Overall, the shape of these signals suggests an exchange process with free alcohol generated in the course of the coordination step of L^1H_2 and the ligands of the dimeric $[Zr_2(OPr^i)_8(HOPr^i)_2]$ precursor.

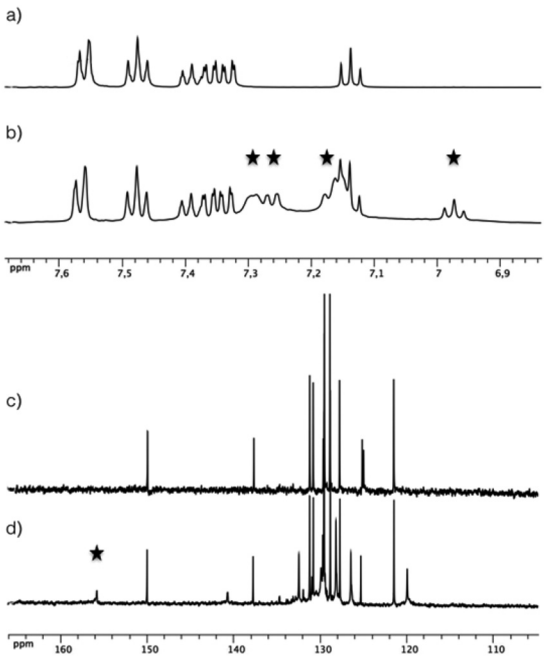

Fig. 2 ^{1}H NMR (a) and ^{13}C NMR (c) of L^1H_2 in CD_2Cl_2 (aromatic region). ^{1}H NMR (b) and ^{13}C NMR (d) of the mixture resulting from the reaction of $[Zr(OPr^i)_4(HOPr^i)]$ with two equivalents of L^1H_2 in CD_2Cl_2 (aromatic region). Signals marked with the star correspond to selected signals attributed to the complex formed *in situ*.

A single deshielded signal (δ = 155.0 ppm) was observed by ^{13}C NMR spectroscopy (Fig. 2c and d), in the region corresponding to a chemical shift typical to the C–O–Zr resonance.[10] Consequently, this ^{13}C NMR spectrum is in full accordance with the formation of a single highly symmetrical complex in solution. It is worth noticing that this complex appears to be unstable in solution as the ^{1}H NMR aromatic region spectrum of a mixture analysed after one day of its preparation reveals only the presence in solution of the initial L^1H_2 molecule.

Among all the available analytical techniques permitting to evaluate the nature of self-assembled architectures or coordination compounds, Diffusion Ordered Spectroscopy (DOSY) experiments[11] are becoming increasingly popular to elucidate these metallo-supramolecular complexes. In the absence of structural data for a given species, this non-invasive technique permits to gain crucial information about the size and the shape of a compound in solution since the diffusion coefficients measured in the course of a DOSY experiment are correlated to the hydrodynamic radius (R_h) of the species in solution according to the Stokes–Einstein equation.[12] Therefore, DOSY became a routine technique to analyse metallo-supramolecular aggregates in solution.[13] For instance, this NMR method has been successfully applied to analyse helicates,[14] cyclic inorganic clusters,[15] cages,[16] rotaxanes,[17] catenanes[18] or metallo-prisms.[19] Thus, DOSY appeared to us as a well adapted technique to analyse the mixtures obtained when Zr(IV) reacts with L^1H_2 and later with L^2H_4. Table 1 gathers the diffusion coefficients measured for the species in solution and

Table 1 Diffusion coefficients in $\mu m^2\ s^{-1}$ measured at room temperature from the mixtures of L^1H_2 or L^2H_4 with $[Zr(OPr^i)_4(HOPr^i)]$. Diffusions are given for measurement in CD_2Cl_2. R_h values are calculated from these diffusions. The R_h values are determined according to the Stokes–Einstein equation with $\eta = 4.603 \times 10^{-4}$ Pa s at 298 K for the viscosity of CD_2Cl_2. The diffusion and R_h are given at ±10%. Let's recall for the previously reported titanium complexes that isopropanol ligands are decoordinated at room temperature for these two complexes in solution. The diffusions given for L^1H_2 or L^2H_4 in CD_2Cl_2 are determined in CD_2Cl_2

Complex in solution	Diffusion ($\mu m^2\ s^{-1}$)	R_h (Å)
$[ZrL^1{}_3H_2]^a$	680	7.0
$[Zr_2L^2{}_3H_4]^b$	505	9.4
References		
L^1H_2	1150	4.1
L^2H_4	830	5.7
$[Ti(L^1)_2(HOPr^i)_2]$[4]	780	6.1
$[Ti_2(L^2)(L^2H)(OPr^i)(HOPr^i)]_2$ [5]	630	7.5

[a] The following stoichiometry has been applied to generate the complex *in situ*: $2L^1H_2 + [Zr(OPr^i)_4(HOPr^i)]$. [b] The following stoichiometry has been applied to generate the complex *in situ*: $L^2H_4 + [Zr(OPr^i)_4(HOPr^i)]$.

the diffusion coefficients measured for the previously reported Ti(IV)-based references. These references were synthesized by using analogous conditions as those reported here. For the experiment conducted with two equivalents of L^1H_2 and one equivalent of $[Zr(OPr^i)_4(HOPr^i)]$, only two species containing aromatic protons are detected by DOSY; L^1H_2 and a new species assumed for being a Zr(IV)-complex (see the ESI†). The diffusion measured for the complex corresponds only to aromatic proton resonances showing that the Zr(IV) ion is not coordinated to isopropanol or isopropoxo ligands. The complex formed *in situ* is around 4.7 times more voluminous than the L^1H_2 compound (estimated volumes: V(Zr(IV)-complex) = 1420 Å^3, $V(L^1H_2)$ = 300 Å^3, where V is calculated from R_h values with the relation $V = 4/3{\cdot}\pi{\cdot}R_h{}^3$ assuming a spherical shape of the molecules). A volume ratio of 1.5 is found between the Zr(IV)-based complex in solution and a previously reported complex with V(Zr(IV)-complex) = 1420 Å^3 and $V([Ti(L^1)_2(HOPr^i)_2])$ = 940 Å^3 highlighting a Zr(IV)-complex containing three ligands. Finally, electrospray ionization mass spectrometry (ESI-MS) analysis allows the unambiguous identification of the complex. As shown in Fig. 3, two intense peaks are detected by ESI-MS. According to the peak observed at high m/z (m/z = 1123.2561), a formula $[ZrL^1{}_3H_2]$ could be proposed for this Zr(IV)-based compound formed *in situ*.

$Zr_2L^2{}_3H_4$

Having determined the formula of the Zr(IV) complex formed *in situ* with L^1H_2, the reaction involving the L^2H_4 proligand was studied. In this case, L^2H_4 reacts with one equivalent of $[Zr(OPr^i)_4(HOPr^i)]$ at room temperature. Neither ^{1}H NMR nor ^{13}C NMR analysis permitted us to extract useful information about the species formed *in situ*. The ^{1}H NMR spectrum indicates the presence of unreacted L^2H_4 in solution with also the presence of large and complex broad signals in the aromatic region too complex to be analysed (see the ESI†). Herein, the coordination process is rather efficient. A conversion of 87% was estimated by integrating the *para*-phenylene bridge proton signal of the unreacted L^2H_4 (δ = 7.68 ppm, singlet) and the methine proton signal (δ = 3.93 ppm, broad septuplet). The ^{13}C NMR spectrum only displays signals relative to L^2H_4 in the region of aromatic carbons. By DOSY, in addition to the diffusion attributed to the unreacted L^2H_4 strand, only one diffusion associated to the formation of a Zr(IV)-based assembly incorporating the ligand L^2 is noticed for the analysed solution. This observation highlights the high selectivity of the self-assembly process. Indeed in this particular case, the molecular volumes could not be estimated accurately for this species, as the shape of the complex in solution is unknown.

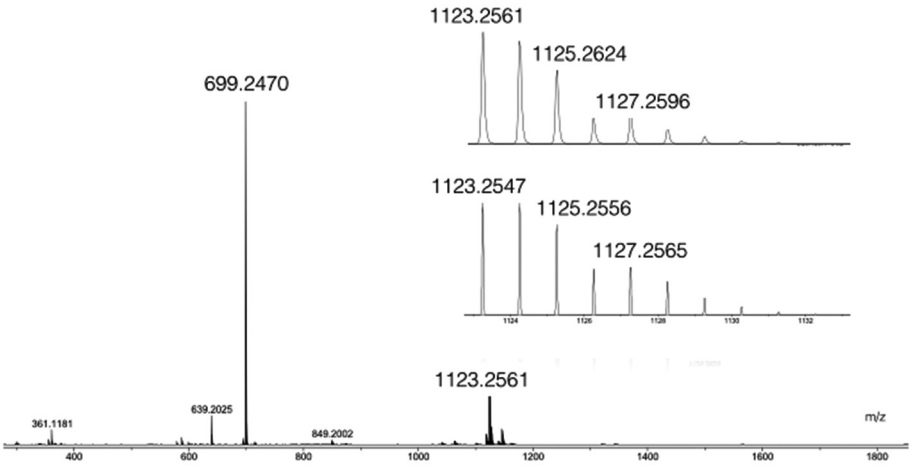

Fig. 3 ESI mass spectrum of the mixture obtained after mixing two equivalents of L^1H_2 with $[Zr(OPr^i)_4(HOPr^i)]$ in CD_2Cl_2. The experimental peak (top) at m/z = 1123.2561 is shown in the insert picture with the isotopic profile (bottom) simulated for $[ZrL^1{}_3H_2 + Na]^+$ (calcd for $C_{72}H_{50}NaO_6Zr$; m/z = 1123.2547). The peak at m/z = 699.2470 is attributed to $[2L^1H_2 + Na]^+$ (calcd for $C_{48}H_{36}NaO_4$; m/z = 699.2511).

However, owing to the order of magnitude of the R_h values (see Table 1), it appears that the Zr(IV)-based assembly is more voluminous than the titanium(IV) dinuclear double stranded helicate already reported.[5] ESI-MS analysis of the crude mixture proves the formation of a dinuclear assembly built up from three strands. The ESI-MS mass spectrum and the simulated isotopic profile for the peak at m/z = 2006.4081 are shown respectively in Fig. 4a and b. The two more intense peaks at m/z = 1214.4673 and m/z = 1813.6810 are originated from LH_4. Peaks at m/z = 1984.4188 and 2006.4081 are attributed to a species formed by two zirconium ions and three strands. In addition to these parent peaks, a peak at m/z = 1898.5531 is detected. This peak is originated from a monomeric complex bearing two strands partially protonated and one strand fully protonated ($[ZrL^2{}_3H_8(H_2O)]^+$). Now, the dinuclear architecture formed *in situ* could be assigned as $Zr_2L^2{}_3H_4$. This result is in agreement with the conclusion made for the experiment conducted with the L^1H_2 ligand.

Molecular modeling

In order to gain detailed information about the Zr(IV)-based architectures generated from L^1H_2 and L^2H_4, molecular models were computed and their energies minimized using density functional theory (DFT) with the hybrid exchange correlation functional B3LYP. The structures of the mononuclear and dinuclear complexes were modelled on the basis of the conclusion drawn by the DOSY experiments and the mass spectrometry analysis. The monomeric complex is designed knowing that the metallic centre is linked to three bidentate ligands. Owing to the reason that in this complex two phenol sub-units compose the Zr(IV) coordination sphere, the three

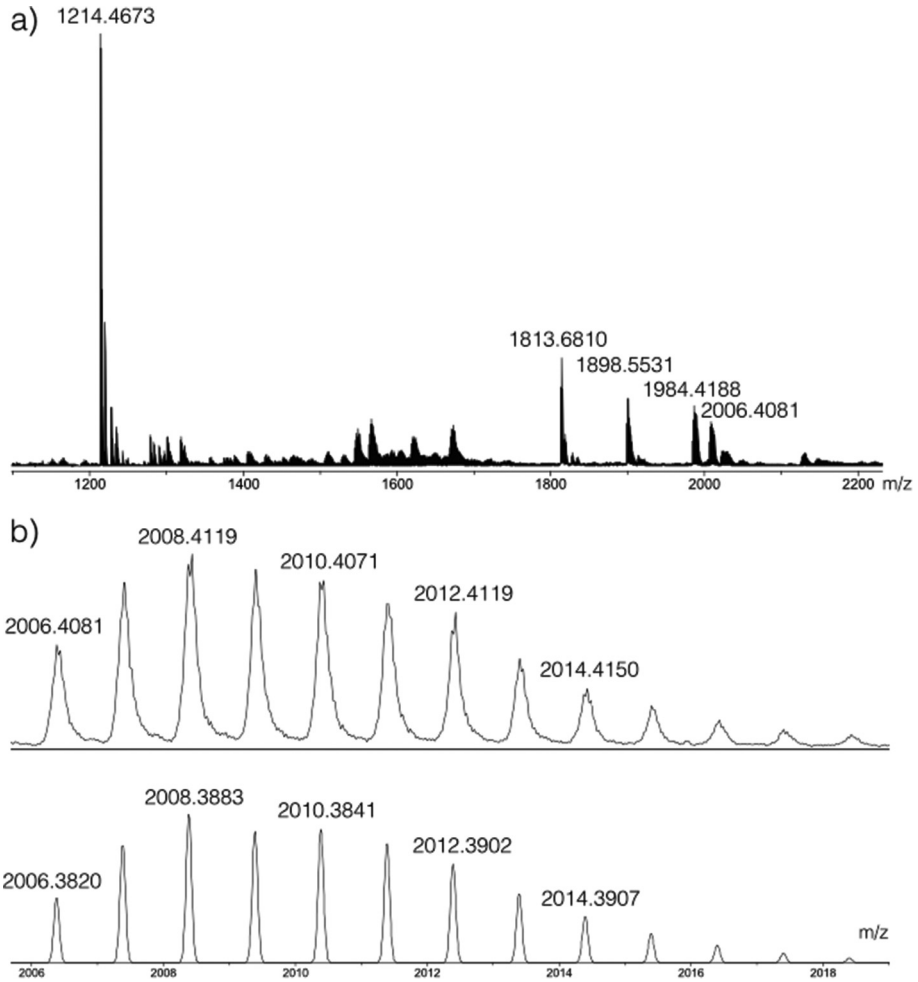

Fig. 4 (a) ESI mass spectrum of the mixture obtained after reacting two equivalents of L^2H_4 with $[Zr(OPr^i)_4(HOPr^i)]$ in CD_2Cl_2. Peaks at m/z = 1214.4673 and 1813.6810 are attributed to L^2H_4 (calcd for $[3L^2H_4 + H_2O]^+$ = 1813.6566 and calcd for $[2L^2H_4 + H_2O]^+$ = 1214.4388). Peaks at m/z = 1984.4188 and 2006.4081 correspond to an assembly incorporating two Zr(IV) centres and three L^2 ligands (calcd for $[Zr_2L^2{}_3H_4(H_2O)]^+$ ($C_{126}H_{84}O_{13}Zr_2$) = 1984.4040 (see the ESI† for the isotopic simulation) and calcd for $[Zr_2L^2{}_3H_4(H_2O)Na]^+$ ($C_{126}H_{83}NaO_{13}Zr_2$) = 2006.3825). The simulated isotopic profile for the $C_{126}H_{83}NaO_{13}Zr$ formula (bottom) and the enlargement of the peak (top) at m/z = 2006.4081 are given in (b). The peak at m/z = 1898.5531 is assigned to $[ZrL^2{}_3H_8(H_2O)]^+$ (calcd for $C_{126}H_{88}O_{13}Zr$, m/z = 1898.5272) (simulated isotopic profile is given in the ESI†).

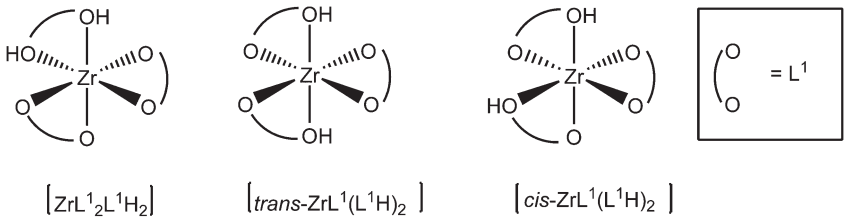

Fig. 5 Schematic representation of the three isomers simulated for $[ZrL^1{}_3H_2]$.

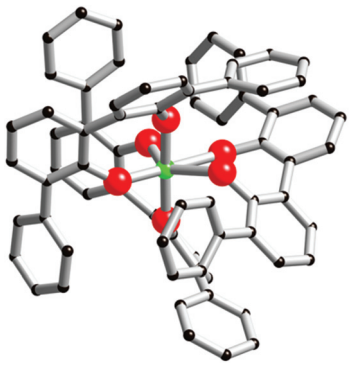

Fig. 6 Computer model of $[cis\text{-}ZrL^1(L^1H)_2]$. The zirconium atom is green, oxygen atoms are red and carbon atoms are black. For these two models, hydrogen atoms are omitted for clarity.

structures $[ZrL^1{}_2L^1H_2]$, $[cis\text{-}ZrL^1(L^1H)_2]$ and $[trans\text{-}ZrL^1(L^1H)_2]$ were optimized (a schematic representation of these isomers is shown in Fig. 5). The calculated structure corresponding to $[cis\text{-}ZrL^1(L^1H)_2]$ is presented in Fig. 6, and the structures of $[ZrL^1{}_2L^1H_2]$ and $[trans\text{-}ZrL^1(L^1H)_2]$ are shown in the ESI.†

The $[cis\text{-}ZrL^1(L^1H)_2]$ isomer appears to be the most stable structure. The energetic difference between $[cis\text{-}ZrL^1(L^1H)_2]$ and $[trans\text{-}ZrL^1(L^1H)_2]$ is found to be 39 kJ mol^{-1}, while between $[cis\text{-}ZrL^1(L^1H)_2]$ and $[ZrL^1{}_2L^1H_2]$ an energy difference of 47 kJ mol^{-1} is determined. As shown in Fig. 6, the $[cis\text{-}ZrL^1(L^1H)_2]$ model indicates that the metallic centre is large enough to accommodate the three ligands leading to a metallic coordination sphere composed of six oxygen atoms. As expected the Zr–O bond lengths are not equivalent as $Zr\text{–}O_{(phenolato)}$ bonds ($Zr\text{–}O_{(phenolato)}$ = 2.01 ± 0.03 Å) are shorter comparatively to $Zr\text{–}O_{(phenol)}$ bonds ($Zr\text{–}O_{(phenol)}$ = 2.35 ± 0.005 Å). From the optimized structure, the R_h has been estimated with the PACHA software.[20] The computed R_h determined for $[cis\text{-}ZrL^1(L^1H)_2]$ is the average between a maximum value corresponding to the longest distance from the barycentre of the molecule and a minimum value $R_{min} = (3V/4\pi)^{1/3}$ derived from the molecular volume[21] (van der Waals radii used: H = 1.2 Å, C = 1.7 Å, O = 1.52 Å,[22] and Zr = 2.00 Å (assumed)). The estimated R_h value (R_h = 7.56 ± 0.4 Å) is in good agreement with the one determined experimentally by DOSY for $[ZrL^1{}_3H_2]$ (R_h = 7.00 ± 0.7 Å).

Next, the computed models incorporating the bis-2,2′-biphenolato strand were calculated. Herein, the modelled structures concern dinuclear species surrounded by three strands. These complexes display to be having the $Zr_2L^2{}_2L^2H_4$ formula. In these structures, we imposed the full protonation of one L^2 strand. As two stereoisomers have to be considered when a dinuclear triple stranded architecture is discussed, the helicate and the mesocate structures[23] were optimized. The models of these two isomers are shown in Fig. 7. The helicate is a much more stable architecture comparatively to the mesocate. An energy difference of 368 kJ mol^{-1} in favour of the $Zr_2L^2{}_2L^2H_4$ triple-stranded helicate was found. In the case of the mesocate, the ligand L^2 appears to be not flexible enough to permit the formation of such an isomer without any constraint. This is illustrated by the angle of 149.63° for $C_{74}\text{–}C_{68}\text{–}C_{59}$ measured in the computed structure, whereas an almost perfect alignment of these carbons is expected (carbons C_{74}, C_{68}, C_{59} are labelled in Fig. 7b). In the case of the helicate structure, the measured angles and distances are reasonable and do not reflect strong constraints for the three L ligands. For the $[Zr_2L^2{}_2L^2H_4]$ helicate, an estimated intermetallic distance of 8.5 Å is measured. The three organic strands wrap around the two zirconium atoms leading to an ovoid shape for the molecule. As it is noticed for $[cis\text{-}ZrL^1(L^1H)_2]$, the $Zr\text{–}O_{(phenol)}$ bonds are much longer than the $Zr\text{–}O_{(phenolato)}$ bonds ($Zr\text{–}O_{(phenol)}$ = 2.35 ± 0.04 Å; $Zr\text{–}O_{(phenolato)}$ = 2.01 ± 0.04 Å). By using the same procedure as the one used for the theoretical R_h value of $cis\text{-}[ZrL^1(L^1H)_2]$, a computed hydrodynamic radius of R_h = 9.7 ± 0.5 Å is determined from the model of the $[Zr_2L^2{}_2(L^2H_4)]$ helicate. Again, this computed radius is in good agreement with the one observed by DOSY for the complex in solution (R_h = 9.4 ± 0.9 Å).

Crystal structure

Having evidenced the formation of defined architectures formed *in situ* when L^1H_2 or L^2H_4 react with $[Zr(OPr^i)_4(HOPr^i)]$, solid-state characterisation of these zirconium-based compounds was undertaken. Crystals suitable for X-ray diffraction analysis were obtained only in the case of ligand L^2H_4. Few white crystals were isolated after several weeks when vapours of diethylether were allowed to slowly diffuse in a dichloromethane solution composed of L^2H_4 (3 eq.) and $[Zr(OPr^i)_4(HOPr^i)]$ (2 eq.). The molecular structure obtained from X-ray diffraction analysis is shown in Fig. 8. The bond valence sum[24] permitted addition of several missing H-atoms not located during refinement of the structure and the complex formula $[Zr_4(L^2)_2(L^2H)(\mu_2\text{-}OH)_5(HO^iPr)_3]$ could be

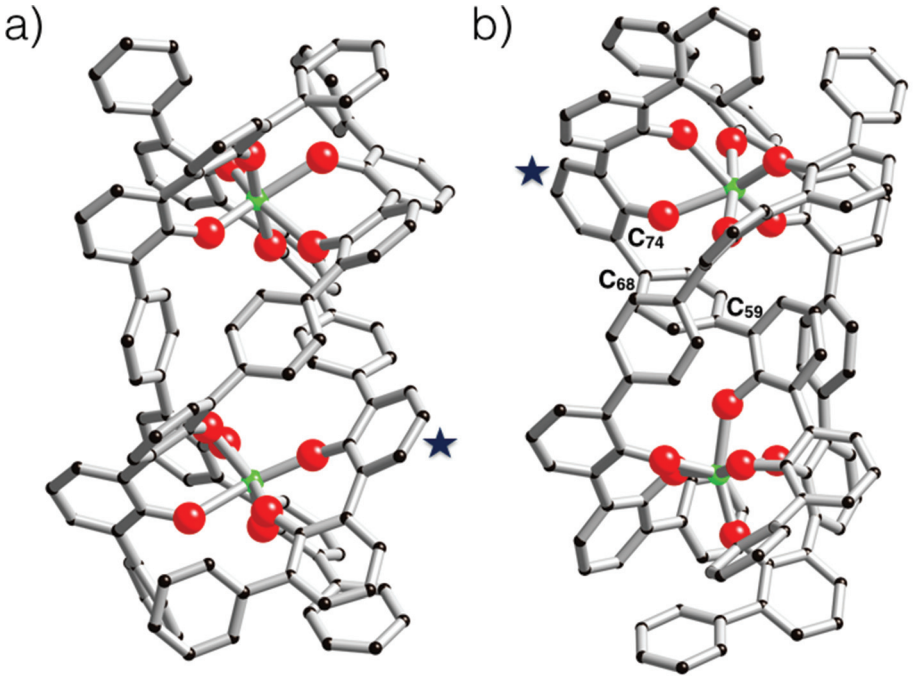

Fig. 7 (a) Computer model of the $[Zr_2L^2{}_2(L^2H_4)]$ helicate. In this model, one strand is fully protonated, and this strand is marked with a star. The computed structure represents the *P*-Δ, Δ enantiomer. (b) Computer model of the $[Zr_2L^2{}_2(L^2H_4)]$ mesocate. In this model, one strand is fully protonated, this strand is marked with a star. This assembly contains a Δ and a Λ subunit. The angle measured between C_{74}–C_{68}–C_{59} is 149.63°. In these models four protons are linked to four oxygen atoms belonging to the same ligand. Zirconium(IV) atoms are green, oxygen atoms are red and carbon atoms are black. For these two models, hydrogen atoms are omitted for clarity.

proposed. Importantly, this species was not detected by ES-MS in the course of the liquid state investigation. The $[Zr_4(L^2)_2(L^2H)(\mu_2\text{-}OH)_5(HO^iPr)_3]$ complex incorporates three strands with one phenol group belonging to the L^2H strand that is not coordinated to a zirconium centre. The three strands are wrapped around a zirconium hydroxo-ladder composed of four metallic centres. This particular arrangement leads to a helical architecture. Each zirconium centre is 6-fold coordinated with pseudo-octahedral coordination geometry as revealed by continuous shape measurements (Zr1(CShM) = 1.615; Zr2(CShM) = 2.756, Zr3(CShM) = 2.317; Zr4(CShM) = 1.1182).[25] Four zirconium atoms form the inorganic core of the complex. The two central metallic atoms (Zr2 and Zr3) are μ_2-hydroxo bridged by one another and are also respectively di-μ_2-hydroxo bridged with a terminal zirconium(IV) centre (Zr1 or Zr4). Also, we notice that two and one isopropanol molecules coordinate with Zr1 and Zr4 respectively. It is noteworthy that the chain-like structure adopted by the inorganic core of the complex is rather original[26] in comparison with the zirconium hydroxo- or oxo-clusters already reported. Here, the chain-like structure contrasts with the spherical or ovoid shapes of the inorganic cores usually found in zirconium-based aggregates.[27] Undoubtedly, the chain-like structure found in $[Zr_4(L^2)_2(L^2H)(\mu_2\text{-}OH)_5(HO^iPr)_3]$ is templated by the L^2 strands.

The structural difference observed between the structure formed in solution and the one observed in the solid-state is obviously related to the occurrence during crystallization of a partial hydrolysis of some Zr–OPh bonds followed by a classical olation reaction leading to $Zr(\mu\text{-}OH)_2Zr$ bridges. As the occurrence of a $[Zr_2(L^2)_2(L^2H_4)]$ helicate in solution cannot be doubted, the first step could be the hydrolysis of two Zr–OPh bonds allowing the formation of the classical di-μ_2-OH bridge causing departure of the fully protonated ligand (L^2H_4) with addition of two alcohol molecules in order to conserve the sixfold coordination of Zr-atoms:

$$[Zr_2(L^2)_2(L^2H_4)] + 2H_2O + 2ROH \rightarrow [(ROH)_2(L^2H_2)Zr(\mu\text{-}OH)_2Zr(L^2)] + L^2H_4$$

The next step could be a further partial hydrolysis of the (L^2H_2) ligand according to:

$$[(ROH)_2(L^2H_2)Zr(\mu\text{-}OH)_2Zr(L^2)] + H_2O \rightarrow [(ROH)_2(L^2H_3)(\eta^1\text{-}OH)Zr(\mu\text{-}OH)_2Zr(L^2)]$$

The solid-state structure could now be obtained through a single olation reaction between one (L^2H_2)-based and one (L^2H_3)-based hydrolysed dimers assisted by proton transfer between the (L^2H_2) and (L^2H_3) moieties in order to allow for departure of another neutral L^2H_4 ligand:

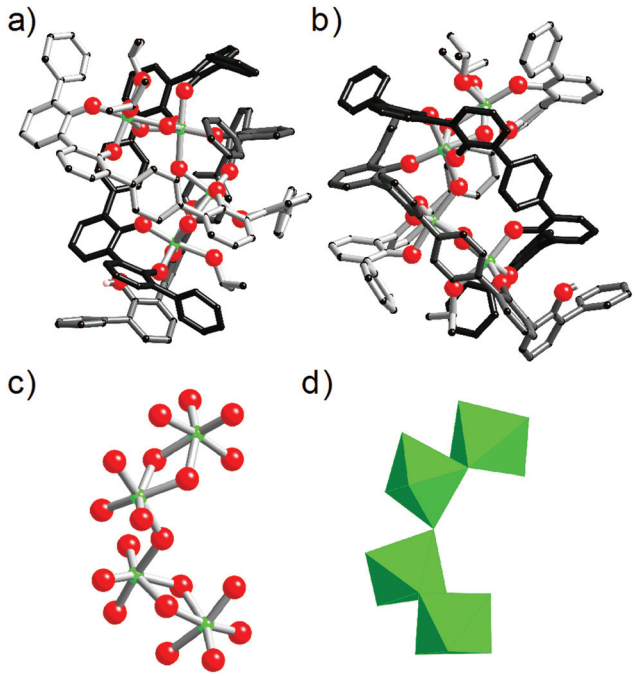

Fig. 8 Two views (a) and (b) of the molecular structure of $[Zr_4(L^2)_2(L^2H)(\mu_2\text{-}OH)_5(HO^iPr)_3]$. In (c) is shown the inorganic core of the structure composed of four pseudo-octahedral ZrO_6 units. (d) Polyhedral model of the inorganic core of the complex. For clarity the three strands are differently coloured and the hydrogen atoms are omitted with the exception of the hydrogen of L^2H. Carbon atoms are in black, oxygen atoms in red and zirconium atoms in green. The disorder of several atoms is not shown.

$$[(ROH)_2(L^2H_2)Zr(\mu\text{-}OH)_2Zr(L^2)] + [(ROH)_2(L^2H_3)(\eta^1\text{-}OH)Zr(\mu\text{-}OH)_2Zr(L^2)] \rightarrow [(ROH)(L^2H)Zr(\mu\text{-}OH)_2Zr(L^2)(\mu\text{-}OH)Zr(\mu\text{-}OH)_2Zr(L^2)(ROH)_2] + ROH + L^2H_4$$

It is worth noticing that this filiation between the solution and the solid-state following the well-established general rules of sol–gel chemistry[28] is in agreement with the following stoichiometric balance:

$$2[Zr_2(L^2)_2(L^2H_4)] + 5H_2O + 3ROH \rightarrow [(ROH)_3Zr_4(\mu\text{-}OH)_5(L^2)_2(L^2H)] + 3L^2H_4$$

One may thus hope that under strictly anhydrous conditions, it could be possible to crystallize the $[Zr_2(L^2)_2(L^2H_4)]$ helicate.

From the structural viewpoint, this scheme supposes a large flexibility of the intermediates, a point that can only be addressed after careful molecular dynamics (MD) studies. However, in the absence of reliable MD potential for zirconium atoms, we have not been able to check this important point. The proposed stoichiometric condensation scheme should thus only be considered as a starting point for full modelling of such a complex condensation process. Another possibility would be that this helicate is indeed a strong acid that could be formulated as a negatively charged $[Zr_2(L^2)_3]^{4-}$ helicate with 4 protons acting as counter-ions and delocalized over the whole structure. These "free" protons would then be able to catalyse the slow condensation of two alcohol molecules with the liberation of one water molecule: ROH + HOR → R–O–R + H_2O. In such a case, the water necessary for the formation of the tetramer would be formed *in situ* preventing the isolation of the helicate in the crystalline state. Further theoretical work is thus needed in order to clarify this point.

Conclusion

We have described herein a coordination chemistry involving one of the most employed zirconium alkoxide precursors, *i.e.* $[Zr(OPr^i)_4(HOPr^i)]$, and two proligands incorporating the 2,2′-biphenol entities. The DOSY investigation supported by mass spectrometry and DFT calculations allowed us to suggest highly plausible structures for the complexes formed *in situ*. The coordination reaction involving the L^1H_2 proligand with Zr(IV) is less efficient comparatively to the one performed with Ti(IV). Nevertheless, we have established that the Zr(IV)-based complex formed from L^1H_2 incorporates three bidentate entities according to DOSY and ESI-MS analysis. DFT calculations indicate the formation of the $[cis\text{-}ZrL^1(L^1H)_2]$ isomer among three possible stereoisomers. Concerning the self-assembled architecture derived from the strand L^2H_4, the DOSY and mass spectrometry analysis proved the formation of a dinuclear assembly formed with three strands. Remarkably, computational modelling proposes an unprecedented triple-stranded helicate structure that incorporates two distorted octahedral ZrO_6 units for the Zr(IV)-assembly. This structure evidence for the complex in solution contrasts strongly with the one obtained for the complex upon crystallization. In this case, a helical architecture constructed around an original chain-like inorganic core displaying the $[Zr_4(L^2)_2(L^2H)(\mu_2\text{-}OH)_5(HO^iPr)_3]$ formula is characterized. It has been proposed that $[Zr_4(L^2)_2(L^2H)(\mu_2\text{-}OH)_5(HO^iPr)_3]$ may in fact be formed during crystallization owing to a partial hydrolysis/condensation reaction of the dimeric helicates mediated by water molecules.

Overall, we have demonstrated the deep impact of the ionic size on the resulting self-assembled architecture formed with the strand L^2 as with Ti(IV) only double-stranded helicates were obtained. Meanwhile, we have shown that the combination of Zr(IV) with the 2,2′-biphenol-based proligands leads to a less effective coordination chemistry to create stable and easily characterized self-assemblies in comparison with the one already developed with Ti(IV).

Experimental part

NMR spectroscopy

Bruker Avance-300, Avance-400 and Avance-500 were used for solution NMR spectroscopic analysis. ^1H NMR DOSY measurements were performed at 500.13 MHz with a 5 mm

^{1}H/X *z*-gradient BBI probe and by applying a PFGSTE pulse sequence using bipolar gradients. DOSY spectra were generated with the DOSY module of NMRNotebook™ software, through maximum entropy and inverse Laplace transform calculations. ^{1}H NMR DOSY measurements were performed at 500.13 MHz with a 5 mm ^{1}H/X *z*-gradient BBI probe and by applying a PFGSTE pulse sequence using bipolar gradients. The solutions were analysed using a NMR microtube. The viscosity of CD_2Cl_2 at 298 K was determined according ref. 5 (see the ESI†). Mass spectrometry was performed at the Service Commun d'Analyses, Université de Strasbourg (France). The electrospray analyses were performed on Micro-TOF (Bruker) apparatus equipped with an electrospray (ES) source. All solvents were dried before use with activated 3 Å molecular sieves. $[Zr(OPr^i)_4(HOPr^i)]$ was purchased from Strem. Ligands were synthesised according to ref. 3. All reactions were performed in a glove bag.

X-ray diffraction

Data were collected on a Bruker SMART CCD diffractometer with Mo Kα radiation. The structures were solved using SHELXS-97 and refined by full matrix least-squares on F^2 using SHELXS-97 with anisotropic thermal parameters for all non-hydrogen atoms. The hydrogen atoms were introduced at calculated positions and not refined (riding model).

Computational details

Density functional theory (DFT) calculations on the different complexes have been performed with the Gaussian09 Revision D01 package.[29] Hybrid exchange correlation functional B3LYP using the LANL2DZ basis set[30–33] with an ultrafine grid was used in all our calculations. Geometry optimization of the $[ZrL^1{}_3H_2]$ and $[Zr_2L^2{}_3H_4]$ complexes started from the crystallographic geometry from either the $[Ti(L^1)_2(HOPr^i)_2]$ (ref. 4) or $[Ti_2(L^2)(L^2H)(OPr^i)(HOPr^i)_2]$ (ref. 5) complexes, where Ti atoms have been replaced by Zr atoms and to which an additional ligand was added. The minimum character of each stationary point was verified by computation of the harmonic vibrational frequencies, which were all real.

$[ZrL^1{}_3H_2]$

The reaction was conducted under a nitrogen atmosphere. In a vial, L^1H_2 (10 mg, 0.03 mmol), and $[Zr(OPr^i)_4(HOPr^i)]$ (6 mg, 0.015 mol) were mixed in dry CD_2Cl_2 (0.75 mL). The resulting uncoloured mixture was analysed by ^{1}H NMR, ^{13}C NMR, DOSY and mass spectrometry. Some signals of the NMR spectrum were attributed to $ZrL^1{}_3H_2$: ^{1}H NMR (CD_2Cl_2, 500 MHz): δ (ppm) = 6.97 (t, 7.5 Hz), 7.26 (bd dd, ^4J = 1.5 Hz, ^3J = 7.5 Hz), 7.29 (bd d); ^{13}C NMR (CD_2Cl_2, 125 MHz): δ (ppm) = 155.8, 140.7, 132.4, 131.9, 130.9, 129.9, 128.2, 126.4, 119.9. ES-MS: m/z = 1123.2561 $[ZrL^1{}_3H_2 + Na]^+$ (calcd for $C_{72}H_{50}NaO_6Zr$; m/z = 1123.2547). DOSY: D = 680 μm^2 s^{-1}.

$[Zr_2L^2{}_3H_4]$

The reaction was conducted under a nitrogen atmosphere. In a vial, L^2H_4 (10 mg, 0.016 mmol), and $[Zr(OPr^i)_4(HOPr^i)]$ (6.45 mg, 0.016 mmol) were mixed in dry CD_2Cl_2 (0.75 mL). The resulting uncoloured mixture was analysed by ^{1}H NMR, ^{13}C NMR, DOSY and mass spectrometry. ^{1}H NMR was too complex to be analysed. ES-MS: m/z = 2006.4081 $[Zr_2L^2{}_3H_4(H_2O)]^+$ (calcd for $C_{126}H_{83}NaO_{13}Zr$ = 2006.3825). DOSY: D = 505 μm^2 s^{-1}.

$[Zr_4(L^2)_2(L^2H)(\mu_2\text{-}OH)_5(HO^iPr)_3]$

The reaction was conducted under a nitrogen atmosphere. Few colourless single crystals were obtained after several weeks by slow vapour diffusion of diethylether on a dry CH_2Cl_2 solution (1.5 mL) composed of L^2H_4 (15 mg, 2.5 10^{-5} mol), and $[Zr(OPr^i)_4(HOPr^i)]$ (6.5 mg, 0.66 eq.).

X-ray data: empirical formula: $C_{285}H_{244}Cl_6O_{45}Zr_8$ $(2(C_{135}H_{100}O_{20}Zr_4)$, $3(C_4H_{10}O)$, $3(CH_2Cl_2)$, $2(H_2O)')$; formula mass: 5331.25 g mol^{-1}; crystal system: triclinic; space group: $P\bar{1}$; unit cell dimensions: a = 17.0968(8) Å, b = 19.1728(8) Å, c = 21.3385(8) Å; α = 81.245(2)°, β = 68.379(2)°, γ = 87.843(2)°, V = 6425.4(5) Å^3; Z = 1; density (calcd): 1.378 g cm^{-3}; crystal size: 0.050 × 0.060 × 0.060 mm^3; θ range for data collection: 1.28 to 30.15°; reflections collected: 33 659; independent reflections: 33 659 [R(int) = 0.0638]; refinement method: full-matrix least squares on F^2; data/restraints/parameters: 33 659/23/1565; goodness-of-fit on F^2: 1.009; final R indices [$I > 2\sigma(I)$]: R_1 = 0.0791, wR_2 = 0.2240; R indices (all data): R_1 = 0.1358, wR_2 = 0.2446. CCDC number: 1451432.

Acknowledgements

This work was done at Université de Strasbourg with public funds allocated by the CNRS, the French government and by the International Center for Frontier Research in Chemistry (icFRC scholarship to G. K.). We thank Dr L. Barloy for fruitful discussions. A. C. is grateful to the HPC centre of the Université de Strasbourg for computer resources. We thank N. Kyritsakas for X-ray structure resolution.

References

1 V. G. Kessler, in *The Sol-Gel Handbook: Synthesis, Characterization and Applications, 3-Volume Set*, John Wiley & Sons, 2015; D. C. Bradley, R. Mehrotra, I. Rothwell and A. Singh, in *Alkoxo and Aryloxo Derivatives of Metals*, Academic Press, San Diego, 2001; Y. Bai, Y. Dou, L.-H. Xie, W. Rutledge, J.-R. Li and H.-C. Zhou, *Chem. Soc. Rev.*, 2016, DOI: 10.1039/C5CS00837A; F. Girardi, L. Fambri, S. Maggini and R. Di Maggio, *J. Appl. Polym. Sci.*, 2015, 41568; S. Gross, *J. Mater. Chem.*, 2011, **21**, 15853; T. J. Boyle, L. A. M. Ottley, S. M. Hoppe and C. F. Campana, *Inorg. Chem.*, 2010, **49**, 10798; G. I. Spijksma, G. A. Seisenbaeva, A. Fischer,

H. J. M. Bouwmeester, D. H. A. Blank and V. G. Kessler, *J. Sol-Gel Sci. Technol.*, 2009, **51**, 10.

2 R. C. Mehrotra and A. Singh, Recent Trends in Metal Alkoxide Chemistry, in *Progress in Inorganic Chemistry*, ed. K. D. Karlin, John Wiley & Sons, Inc., Hoboken, NJ, USA, 1997.

3 C. Diebold, D. M. Weekes, M. T. Navarrete, P. Mobian, N. Kyritsakas and M. Henry, *Eur. J. Org. Chem.*, 2010, 6949.

4 C. Diebold, P. Mobian, C. Huguenard, L. Allouche and M. Henry, *Dalton Trans.*, 2009, **46**, 10178.

5 D. M. Weekes, C. Diebold, P. Mobian, C. Huguenard, L. Allouche and M. Henry, *Chem. – Eur. J.*, 2014, **20**, 5092.

6 R. D. Shannon, *Acta Crystallogr., Sect. A: Cryst. Phys., Diffr., Theor. Gen. Cryst.*, 1976, **32**, 751.

7 L. Cooper, N. Guillou, C. Martineau, E. Elkaim, F. Taulelle, C. Serre and T. Devic, *Eur. J. Inorg. Chem.*, 2014, **36**, 6281; H.-J. Chuang and B.-T. Ko, *Dalton Trans.*, 2015, **44**, 598; N. H. Lee, D. W. Lee, H. Yeo, K. Kwak, H. Sook Chun and K. M. Ok, *CrystEngComm*, 2014, **16**, 5619; M. Steyn, H. G. Visser, A. Roodt and T. J. Muller, *Acta Crystallogr., Sect. E: Struct. Rep. Online*, 2011, **67**, m1240–m1241.

8 A. Stopper, K. Press, J. Okuda, I. Goldberg and M. Kol, *Inorg. Chem.*, 2014, **53**, 9140; M. Sietzen, H. Wadepohl and J. Ballmann, *Organometallics*, 2014, **33**, 612; E. Otten, P. Dijkstra, C. Visser, A. Meetsma and B. Hessen, *Organometallics*, 2005, **24**, 4374; M. P. Gil and O. L. Casagrande, *J. Organomet. Chem.*, 2004, **689**, 286; J. D. Scollard, D. H. McConville and J. J. Vittal, *Organometallics*, 1995, **14**, 5478; E. Y. Tshuva, I. Goldberg and M. Kol, *Organometallics*, 2001, **20**, 3017.

9 B. A. Vaartstra, J. C. Huffman, P. S. Gradeff, L. G. Hubert-Pfalzgraf, J.-C. Daran, S. Parraud, K. Yunlu and K. G. Caulto, *Inorg. Chem.*, 1990, **29**, 3136.

10 L. Azor, C. Bailly, L. Brelot, M. Henry, P. Mobian and S. Dagorne, *Inorg. Chem.*, 2012, 10876.

11 E. L. Hahn, *Phys. Rev.*, 1950, **80**, 580; O. E. Stejskal and J. E. Tanner, *J. Chem. Phys.*, 1965, **42**, 288.

12 E. L. Cussler, *Diffusion: Mass Transfer in Fluid Systems*, Cambridge University Press, Cambridge, 1984.

13 For a general review concerning the applications of DOSY in the field of supramolecular chemistry see: Y. Cohen, L. Avram and L. Frish, *Angew. Chem., Int. Ed.*, 2005, **44**, 520.

14 L. Allouche, A. Marquis and J.-M. Lehn, *Chem. – Eur. J.*, 2006, **12**, 7520.

15 S. Floquet, S. Brun, J.-F. Lemonnier, M. Henry, A. Delsuc, Y. Prigent, E. Cadot and F. Taulelle, *J. Am. Chem. Soc.*, 2009, **131**, 17255.

16 S. Pasquale, S. Sattin, E. C. Escudero-Adán, M. Martínez-Belmonte and J. de Mendoza, *Nat. Commun.*, 2012, **3**, 785; S. Durot, L. Flamigni, J. Taesch, T. T. Dang, V. Heitz and B. Ventura, *Chem. – Eur. J.*, 2014, **20**, 9979; K. Mahata, P. D. Frischmann and F. Würthner, *J. Am. Chem. Soc.*, 2013, **135**, 15656.

17 J. Frey, C. Tock, J.-P. Collin, V. Heitz and J.-P. Sauvage, *J. Am. Chem. Soc.*, 2008, **130**, 4592.

18 A. Westcott, J. Fisher, L. P. Harding, P. Rizkallah and M. J. Hardie, *J. Am. Chem. Soc.*, 2008, **130**, 2950.

19 T. K. Ronson, J. Fisher, L. P. Harding and M. J. Hardie, *Angew. Chem., Int. Ed.*, 2007, **46**, 9086.

20 M. Henry, in *Encyclopedia of Nanoscience and Nanotechnology*, ed. H. S. Nalwa, American Scientific Publishers, 2011, vol. 14, pp. 1–43; H. Senouci, B. Millet, C. Volkringer, C. Huguenard, F. Taulelle and M. Henry, *C. R. Chim.*, 2010, **13**, 69; M. Henry, in *Advances in Quantum Chemical Bonding Structures*, ed. M. V. Putz, Transworld Research Network, Kerala, India, 2009, pp. 153–211; C. Carpanese, S. Ferlay, N. Kyritsakas, M. Henry and M. W. Hosseini, *Chem. Commun.*, 2009, 6786; M. Henry and M. W. Hosseini, *New J. Chem.*, 2004, **28**, 897; M. Henry, *ChemPhysChem*, 2002, **3**, 561; M. Henry, *ChemPhysChem*, 2002, **3**, 607.

21 A. Gavezotti, *J. Am. Chem. Soc.*, 1983, **105**, 5220.

22 A. Bondi, *J. Phys. Chem.*, 1964, **68**, 441.

23 For general reviews on helicates see: M. Albrecht, *Chem. Rev.*, 2001, **101**, 3457; C. Piguet, G. Bernardinelli and G. Hopfgartner, *Chem. Rev.*, 1997, **97**, 2005. For recent examples of triple-stranded helicates see: Q. Li, F. Huang, Y. Fan, Y. Wang, J. Li, Y. He and H. Jiang, *Eur. J. Inorg. Chem.*, 2014, **20**, 3235; C.-S. Tsanga, C.-C. Yeea, S.-M. Yiua, W.-T. Wong and H.-L. Kwong, *Polyhedron*, 2014, **83**, 167; Q. Li, F. Huang, Y. Fan, Y. Wang, J. Li, Y. He and H. Jiang, *Eur. J. Inorg. Chem.*, 2014, **20**, 3235; O. Gidron, M.-O. Ebert, N. Trapp and F. Diederich, *Angew. Chem., Int. Ed.*, 2014, **53**, 13614; C. Gütz, R. Hovorka, N. Struch, J. Bunzen, G. Meyer-Eppler, Z.-W. Qu, S. Grimme, F. Topić, K. Rissanen, M. Cetina, M. Engeser and A. Lützen, *J. Am. Chem. Soc.*, 2014, **136**, 11830; Z. Zhang and D. Dolphin, *Chem. Commun.*, 2009, 6931.

24 I. D. Brown and D. Altermatt, *Acta Crystallogr., Sect. B: Struct. Crystallogr. Cryst. Chem.*, 1985, **41**, 244.

25 D. Casanova, M. Llunell, P. Alemany and S. Alavarez, *Chem. – Eur. J.*, 2005, **11**, 1479.

26 Few zirconium-based aggregates present a chain-like structure: B. Moraru, S. Gross, G. Kickelbick, G. Trimmel and U. Schubert, *Monatsh. Chem.*, 2001, **132**, 993; T. J. Boyle, L. A. M. Ottley and M. A. Rodriguez, *Polyhedron*, 2005, **24**, 1727.

27 For zirconium-based aggregates presenting spherical or ovoid inorganic cores see: S. Yuan, W. Lu, Y.-P. Chen, Q. Zhang, T.-F. Liu, D. Feng, X. Wang, J. Qin and H.-C. Zhou, *J. Am. Chem. Soc.*, 2015, **137**, 3177; C. Artner, M. Czakler and U. Schubert, *Inorg. Chim. Acta*, 2015, **432**, 208; V. Bon, I. Senkovska, M. S. Weiss and S. Kaskel, *CrystEngComm*, 2013, **15**, 9572; P. Piszczek, A. Radtke, A. Grodzicki, A. Wojtczak and J. Chojnacki, *Polyhedron*, 2007, **26**, 679; F. R. Kogler, M. Jupa, M. Puchberger and U. Schubert, *J. Mater. Chem.*, 2004, **14**, 3133; G. Kickelbick, P. Wiede and U. Schubert, *Inorg. Chim. Acta*, 1999, **284**, 1; A. Otero, J. Fernández-Baeza, A. Antiñolo, J. Tejeda, A. Lara-Sánchez, L. Sánchez-Barba, M. Fernández-López and I. López-Solera, *Inorg. Chem.*, 2004, **43**, 1350; M. Y. Reza,

H. Matsushima, M. Koikawa, M. Nakashima and T. Tokii, *Polyhedron*, 1999, **18**, 787.

28 C. Sanchez, J. Livage and M. Henry, *Prog. Solid State Chem.*, 1988, **18**, 259.

29 M. J. Frisch, G. W. Trucks, H. B. Schlegel, G. E. Scuseria, M. A. Robb, J. R. Cheeseman, G. Scalmani, V. Barone, B. Mennucci, G. A. Petersson, H. Nakatsuji, M. Caricato, X. Li, H. P. Hratchian, A. F. Izmaylov, J. Bloino, G. Zheng, J. L. Sonnenberg, M. Hada, M. Ehara, K. Toyota, R. Fukuda, J. Hasegawa, M. Ishida, T. Nakajima, Y. Honda, O. Kitao, H. Nakai, T. Vreven, J. A. Montgomery Jr., J. E. Peralta, F. Ogliaro, M. Bearpark, J. J. Heyd, E. Brothers, K. N. Kudin, V. N. Staroverov, R. Kobayashi, J. Normand, K. Raghavachari, A. Rendell, J. C. Burant, S. S. Iyengar, J. Tomasi, M. Cossi, N. Rega, J. M. Millam, M. Klene, J. E. Knox, J. B. Cross, V. Bakken, C. Adamo, J. Jaramillo, R. Gomperts, R. E. Stratmann, O. Yazyev, A. J. Austin, R. Cammi, C. Pomelli, J. W. Ochterski, R. L. Martin, K. Morokuma, V. G. Zakrzewski, G. A. Voth, P. Salvador, J. J. Dannenberg, S. Dapprich, A. D. Daniels, Ö. Farkas, J. B. Foresman, J. V. Ortiz, J. Cioslowski and D. J. Fox, *Gaussian 09, Revision D.01*, Gaussian, Inc., Wallingford, CT, 2009.

30 T. H. Dunning Jr. and P. J. Hay, in *Modern Theoretical Chemistry*, ed. H. F. Schaefer III, Plenum, New York, 1977, vol. 3, pp. 1–28.

31 P. J. Hay and W. R. Wadt, *J. Chem. Phys.*, 1985, **82**, 270.

32 W. R. Wadt and P. J. Hay, *J. Chem. Phys.*, 1985, **82**, 284.

33 P. J. Hay and W. R. Wadt, *J. Chem. Phys.*, 1985, **82**, 299.